3D NUMERICAL MODELING OF PARAMETRIC SPEAKER USING FINITE-DIFFERENCE TIME-DOMAIN

*Lijun Zhu**

Center for Energy and Geo Processing
Georgia Institute of Technology
Atlanta, GA 30332

Dinei Florencio

Microsoft Research
Redmond, WA 98052

ABSTRACT

Parametric speakers produce sound by emitting ultrasound, and using the small nonlinearity in air to demodulate it back to audible sound. The use of ultrasound allows for producing very narrow audio beams, which finds application in a number of military and consumer scenarios. However, designing better parametric speakers has been hard: closed-form solution of the nonlinear wave equation for generic geometries is nearly impossible, and the only existing solution was derived for the simple case of a cylindrical beam. FDTD methods were considered not practical since the desired (audible) signal is orders of magnitude weaker than the ultrasound signal, and thus the noise floor (from the numerical approximation) will dwarf the audible signal. In this paper, we introduce a novel FDTD scheme that models nonlinear sound propagation for parametric speakers. By taking the difference between linear and nonlinear FDTD simulations, we successfully suppress the numerical noise floor and extract the audible signal. Both spectrum and radiation pattern of simulation match the measurements well. This offers a simulation tool for further research in creating advanced parametric speakers.

Index Terms— parametric speaker, array, FDTD, acoustic, nonlinear

1. INTRODUCTION

Parametric speakers are an intriguing way of producing very directional sound. They produce sound by emitting modulated ultrasound, and using the small non-linearities [**?**] in air to demodulate it back to audible sound. The short wavelength of the ultrasound carrier allows to produce very narrow beams. However, these nonlinearities are small, and the audible sound is typically 60dB or more below the ultrasound carrier. Moreover, for two well collimated sound beams, a virtual end-fire array of the audible signal will form and reinforce the directional audible signal [**?**]. The need to account for the nonlinear distortion, as well as the beamforming aspects of both ultrasound and demodulated signal, make the analysis of parametric speakers array complex. Indeed, early efforts in both underwater [**?**, **?**, **?**, **?**] and airborne [**?**, **?**] scenarios, were focused on either experimental or simple analytical analysis.

Improving 3D in consumer scenarios [**?**, **?**, **?**] with traditional loudspeakers is hard, making parametric speakers particularly appealing [**?**]. This can also be coupled with beam steering and user localization, either based on face tracking or Sound Source Localization [**?**]. Parametric Speakers can also be used to improve Acoustic Echo cancellation [**?**, **?**, **?**]. Highly directional sound sources using piston [**?**] or PZT (lead zirconate titanate) [**?**] were developed using airborne parametric speakers.

Designing better parametric speakers has been challenging: Solving the nonlinear wave equation for generic geometries is nearly impossible, and the existing solution was derived for the simple case of a cylindrical beam. It relies on Khokhlov-Zabolotskaya-Kuznetsov (KZK) equation [**?**, **?**, **?**], which is an simplification of Westervelt equation under parabolic approximation. Although this analytic method gives a good close-form estimation of audible beam [**?**, **?**], the phase array constructed based on this theory has always been troublesome [**?**]. Not only the main lobe of steered array deviates from the designed direction, the side lobes of such array design tend to have considerable energy leak. Moreover, the analytic approximation is only valid for collimated two beams scenario under far-field assumption which limits novel array designs for parametric speakers. A numerical method that directly solves Westervelt equation for a given scenario would greatly help designing advanced parametric speakers. This would allow for novel array designs, more flxible transducer placement, as well as incorporating the effects of the user's head and a room model[**?**, **?**], as it was done in [**?**] for traditional loudspeakers.

Due to its high computational complexity, numerical solutions have been long shunned upon. Indeed, the higher frequencies of ultrasound imply not only a higher sampling rate, but also a finer grid. Yet, with computational power soaring over the past decade, many numerical schemes have been developed for solving partial differential equations. A finite-difference time-domain (FDTD) scheme was proposed recently for medical imaging scenario [**?**]. However, previous methods [**?**, **?**] used in ultrasonic imaging of human bodies are not practical for the case of parametric speakers for a simple reason: the noise floor of numerical methods is typically 20-40dB, which will simply dwarf the desired (audible) signal. In developing a highly directional steerable indoor parametric acoustic source, a novel FDTD scheme for nonlinear acoustic wave is proposed in this study. As we will explain later, we overcome the noise floor problem by computing the results twice: with and without the nonlinearities, and subtracting the results. Because the nonlinearities are so small, they do not affect the noise floor, which is mostly generated by the discrete grid approximation.

The rest of the paper is organized as follows: Section 2 reviews the related theory, including the analytic approximation and existing numerical solutions. In section 3 we discuss our approach to reduce

*The first author performed the work during an internship at Microsoft Research

the noise floor when one is mostly interested in the nonlinear distortion. Finally, Section 4 presents some simulation to validate our method, and Section 5 make final comments.

2. THEORY

2.1. Analytic Approximation

Westervelt [**?**] considered the scattered pressure field of primary waves within a given volume due to the non-linearities in the median as volume distributed sources. Using a quasi-linear approach, Berktay [**?**] gives the expression of differential pressure field at difference frequency at a point (R, θ) in the far field as:

$$p(R,\theta) = \frac{P_1 P_2 \Omega^2 S}{4\pi\rho c^4 R} \exp(-\alpha R) \frac{\cos(\Omega t - KR - \beta)}{\left\{A^2 + \left[2K\sin^2(\theta/2)\right]^2\right\}^{1/2}} \quad (1)$$

where p is the audible pressure field, P_1 and P_2 are the ultrasound pressure amplitudes at the transducer surface, S is the cross-section area of the ultrasound beams, ρ is medium density, c is sound velocity, $A = \alpha_1 + \alpha_2 - \alpha\cos\theta$ α_1, α_2 and α are absorption coefficients of the ultrasound and audible sound respectively, and $\tan\beta = A/[2K\sin(\theta/2)]$.

Berktay's equation gives a closed-form solution to two collimated acoustic beams. It not only includes the wave propagation of ultrasound and audible sound signal but also takes into account the virtual end-fire array form by audible signal in far field generated from nonlinear propagation of the ultrasound beams. More detailed derivation and analysis of such method can be found in [**?**, **?**, **?**]. However, such method relies on a cylindrical assumption and far-field approximation. In cases that near-field effects are considered, the prediction by this method is far from the experiment result as shown in Figure **??**. Thus, a more robust method that can model near-field effects are needed for this application. Numerical solution may provide an alternative, as we'll see next.

2.2. Numerical Solution

Instead of Berktay's equation, one can directly use the Westervelt equation to model the complete nonlinear wave propagation. It takes the following form [**?**]:

$$\triangle p - \frac{1}{c}\frac{\partial^2 p}{\partial t^2} + \frac{\delta}{c^4}\frac{\partial^3 p}{\partial t^3} + \frac{\beta}{\rho c^4}\frac{\partial^2 p^2}{\partial t^2} = 0 \quad (2)$$

where $\triangle$ is Laplace operator, δ is the acoustic diffusivity and $\beta = 1 + B/2A$ is the nonlinearity coefficient. The first two terms in equation (**??**) describe the lossless acoustic wave propagation. The third term models loss due to the viscosity and the heat conduction in the media fluid. The forth term describes the nonlinear effects. The third term is dropped due to the relatively low viscosity in air. Thus, the above equation reduces to

$$\triangle p - \frac{1}{c}\frac{\partial^2 p}{\partial t^2} + \frac{\beta}{\rho c^4}\frac{\partial^2 p^2}{\partial t^2} = 0 \quad (3)$$

By neglecting the nonlinear effect, it further reduces to

$$\triangle p - \frac{1}{c}\frac{\partial^2 p}{\partial t^2} = 0 \quad (4)$$

for linear wave propagation.

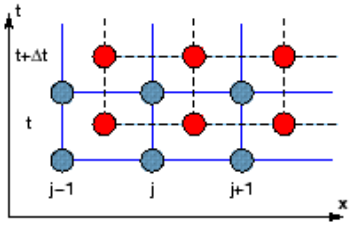

Fig. 1. 1D Yee grid in FDTD scheme with both space and time discretization.

FDTD solves partial differential equations by discretizing the space and time using an Yee grid [**?**] (see Fig. **??**) and approximating derivatives with higher order finite differences. In section **??** and **??**, approximation of time derivatives ($\frac{\partial^2 p}{\partial t^2}$ and $\frac{\partial^2 p^2}{\partial t^2}$) and space derivatives ($\triangle p$) in equation (**??**) and (**??**) are discussed separately.

2.2.1. *Temporal Derivatives and Update Equations*

The time derivatives are approximated in [**?**] as following :

$$\frac{\partial^2 p}{\partial t^2} \approx \frac{1}{(\triangle t)^2}(p^{n+1}_{i,j,k} - 2p^n_{i,j,k} + p^{n-1}_{i,j,k}) \quad (5)$$

and

$$\begin{aligned}\frac{\partial^2 p^2}{\partial t^2} &= 2\left(\frac{\partial p}{\partial t}\right)^2 + 2p\frac{\partial^2 p}{\partial t^2} \\ &\approx \frac{2}{(\triangle t)^2}[(p^n_{i,j,k} - p^{n-1}_{i,j,k})^2 \\ &\quad + p^n_{i,j,k}(p^{n+1}_{i,j,k} - 2p^n_{i,j,k} + p^{n-1}_{i,j,k})] \end{aligned} \quad (6)$$

Indices i, j, and k denote the spatial dimensions x, y, and z respectively. n indexes the time dimension. $\triangle t$ is the finite difference between two temporal samples. Equations (**??**) and (**??**) can be substituted into equations (**??**) and (**??**) to get an temporal update equation for both linear and nonlinear propagation as shown in equation (**??**) and (**??**) respectively.

$$p^{n+1}_{i,j,k} = (c\triangle)^2[\triangle p + s(t)] + 2p^n_{i,j,k} - p^{n-1}_{i,j,k} \quad (7)$$

$$\begin{aligned} p^{n+1}_{i,j,k} &= (c\triangle t)^2[\triangle p + s(t)] + 2p^n_{i,j,k} - p^{n-1}_{i,j,k} \\ &\quad + \frac{2\beta}{\rho c^2}\frac{(p^{n-1}_{i,j,k})^2 - p^{n-1}_{i,j,k}p^n_{i,j,k} - (p^n_{i,j,k})^2}{1 - \frac{2\beta}{\rho c^2}p^n_{i,j,k}} \end{aligned} \quad (8)$$

where $\triangle p$ is the spatial derivative whose numerical approximation will be given shortly after and $s(t)$ is the addictive source signal.

2.2.2. *Spatial Derivatives and Perfect Matched Layers*

Unlike the numerical approximation of the spatial derivatives given by [**?**], convolutional perfect matched layer (CPML) method [**?**] is used to absorb wave energy on the boundaries and avoid undesired reflection. To implement this CPML method, two auxiliary fields A and P are used as intermediate variables of taking derivatives of pressure field p. Here we define $A_h = \frac{\partial p_h}{\partial h}$ and $P_h = \frac{\partial A_h}{\partial h}$ where h represenet x, y, or z. To add adsorption into the acoustic wave equation, we need to insert two convolutional variables Φ and Ψ

for auxiliary fields A and P respectively. Thus, we have $\triangle p = P_x + P_y + P_z$. The explicit relationship between these variables are shown below:

$$\begin{cases} A_h = \frac{\partial p}{\partial h} + \Phi_h \\ P_h = \frac{\partial A}{\partial h} + \Psi_h \\ \Phi_h^{n+1} = b_h \Phi_h^{n-1} + (b_h - 1)\frac{\partial^n P_h}{\partial h} \\ \Psi_h^{n+1} = b_h \Psi_h^{n-1} + (b_h - 1)\frac{\partial^n A_h}{\partial h} \end{cases} \quad (9)$$

where the absorption coefficient $b_h = e^{-d_h \triangle t}$. Here, d_h is damping factor.

In this method, damping factor d_h controls the rate of acoustic wave attenuation in the media. In the PML, d_h gradually increases away from the boundary while it stay constant in the region of interest. There is a trade-off between damping (PML length) and reflection (simulation result). The slower damping (longer PML length), the weaker artificial reflection signal strength; however, it requires longer computation time and large memory. The PML damping factor we used here is a function of PML length L and depth in PML from boundary h_d as following:

$$d_h = a\frac{h_d}{L} \quad (10)$$

where $a = c\frac{\log(\alpha)}{L}$ and α is a parameter that can be set for specific scenario. In this study, $\alpha = 10^{-6}$ is used. A detailed discussion on non-reflective PML can be found in [**?**].

2.2.3. Discretization and Stability of FDTD

FDTD method discretizes space and time and solve wave equation on a sufficiently small element. This raises questions on the minimum spacial and temporal sampling rate. If we define the smallest spatial element in FDTD as

$$dh = \frac{\lambda_{min}}{n} \quad (11)$$

The Nyquist rate of $n = 2$ may cause numerical dispersion in FDTD scheme as shown in [**?**]. For fourth order differentiators used in this study, the empirical requirements in [**?**] is $n \leq 8$. On the other side, the temporal sampling rate depends on dh and is governed by Courant-Friedrichs-Lewy condition [**?**] shown below:

$$dt \leq \frac{dh}{h\sqrt{3}c} \quad (12)$$

where the parameter $h = 7/6$, as given in [**?**].

3. EXTRACTING DIFFERENCE SIGNAL FROM FDTD SIMULATION

Although higher harmonics generated from nonlinear wave propagation can be successfully modeled by FDTD as shown in [**?**], there is one problem of using the same FDTD to model parametric speakers. The numerical noise floor of typical FDTD simulation is about 25 dB below the ultrasound wave as shown in Fig. **??**(a) while the audible signal is roughly 65 dB below the ultrasound wave in experiments shown in Fig. **??**(b). Thus, the FDTD method proposed in [**?**] cannot be directly applied to parametric speakers without modification.

Since linear wave propagation dominates the nonlinear case (they almost overlap in Figure **??**(a)), most of the numerical error comes from the approximations in the linear propagation. As such, we assume that the linear (**??**) and nonlinear (**??**) FDTD schemes share similar numerical error since the grid densities of both cases are the same, and the signals are nearly identical. Thus, subtracting linear simulation from the nonlinear simulation will cancel most of the numerical error. This will lower the numerical noise floor for the signal of interest (the difference signal), and thus the audible signal can be extracted from the FDTD simulation.

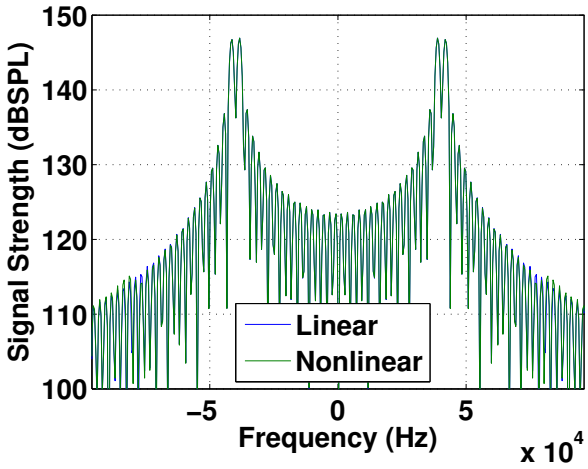

(a) Linear vs. nonlinear spectrum

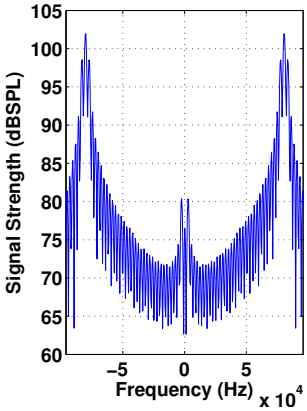

(b) Difference (full)

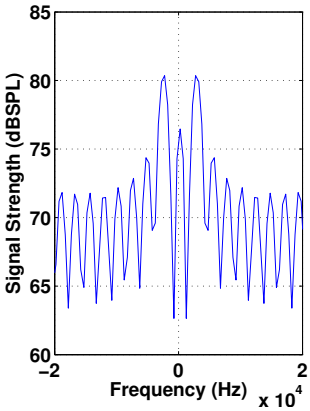

(c) Difference (audible)

Fig. 2. Simulation results of a 39KHz and 41Khz colimated beams. (a) Spectrum of linear and nonlinear simulation from FDTD method. Note how similar the two are; (b) Spectrum of difference signal between the linear and nonlinear simulations in full frequency band. Note the audible signal (around 2KH) is now above the noise floor; (c) Spectrum of difference signal between linear and nonlinear simulations zoomed in for audible frequency band.

4. VALIDATION

In this section, acoustic pressure fields generated from analytic approximation and numerical solution are compared with the measured pressure field to verify the FDTD simulation results. Two sound beams of frequency 39 kHz and 41 kHz are transmitted by an 8 by

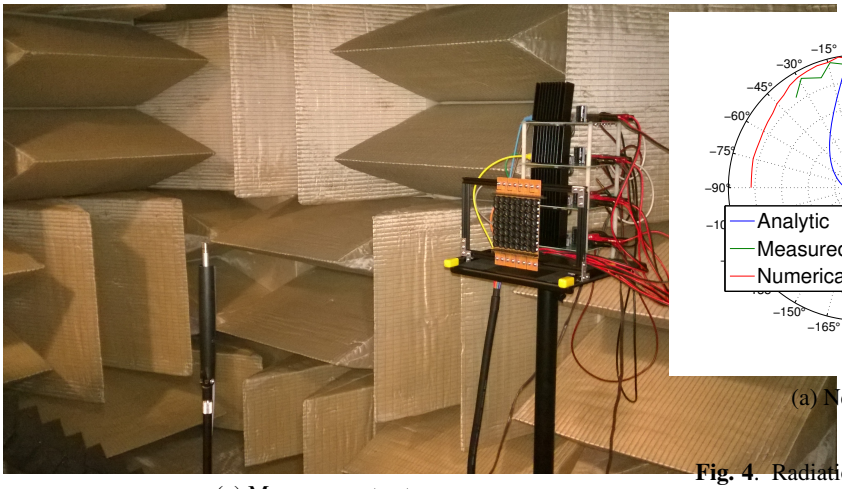

(a) Measurement setup

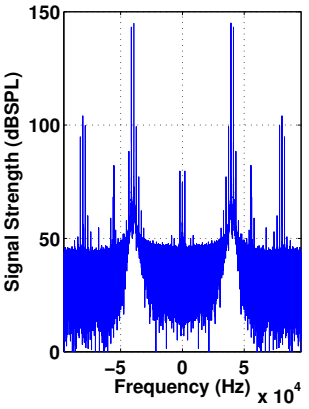

(b) Measured Spectrum

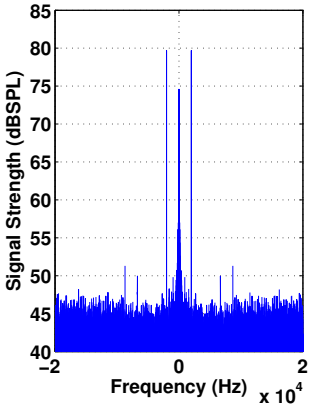

(c) Measured Spectrum(audible)

Fig. 3. Measurement results: (a) measurement setup for an 8 by 8 parametric speaker array in anechoic chamber using a 1/4 in B & K reference microphone; (b) measured spectrum of this parametric speaker array; (c) measured spectrum zoomed in for audible frequency band.

8 parametric array and measured by a 1/4 inch B & K reference microphone in an anechoic chamber as shown in Fig. **??**(a). Each transducer element is 10 mm in diameter and 5 mm thick. All the environment constants in both analytic and numerical simulation are assumed in 20°C, 1 atmosphere pressure.

Fig. **??**(a) shows the spectrum of those two beams simulated by FDTD under linear propagation and nonlinear propagation assumption. Both spectra have noise floors about 20 dB below signal which are higher than the magnitude of audible signal measured in Fig. **??**(b). However, taking the difference between those two simulated signals, the audible signal is extracted as shown in Fig. **??**(b) with correct frequency and amplitude comparing to the measured spectrum shown in Fig. **??**(b). Moreover, the linear and nonlinear spectrums are very similar in Fig. **??**(a). This indicates that most of the energy propagation by this acoustic wave is through linear propagation. It opens up the door to design a hybrid simulation that uses conventional array beam forming method for long distance, non-

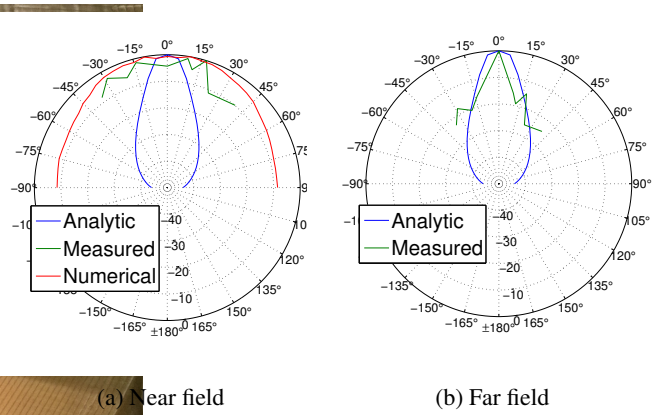

(a) Near field (b) Far field

Fig. 4. Radiation pattern comparison between analytic approximation, measurement, and numerical solution in both (a) near field and (b) far field scenario.

collimated ultrasound linear propagation and passes the boundary conditions to FDTD to have an accurate simulation in the intersection of sound beam under nonlinear wave propagation assumption.

Notice that in Fig. **??**(b), there are three strong components around 80 kHz. These signals' frequencies are 78 kHz, 80 kHz and 82 kHz and they are corresponding to the second harmonic of 39 kHz, summation frequency signal, and second harmonic of 41 kHz as predicted by Westervelt's theory [**?**]. The corresponding signals show up in FDTD simulation in Fig. **??**(b) with the same magnitudes. This shows that, as expected, the higher harmonic components can also be correctly modeled by FDTD. For analysis of higher harmonics modeling, more detailed results can be found in [**?**].

Due to the limitation of computation resource, FDTD was used only for near-field simulation. Fig. **??** shows the comparison of radiation pattern between analytic approximation, measurement, and FDTD solution. Although analytic approximation give a good prediction of radiation pattern in far field, it fails to predict that in near field where the numerical method can give a good approximation of radiation pattern.

5. CONCLUSION

Parametric speaker are a promising solution to improve the quality and experience of personal sound. However, difficulties in analysing new array architectures have long held progress in the development of novel, more effective designs. In this paper, we have introduced a new FDTD method to model the nonlinear acoustic wave propagation for parametric speakers. Unlike previous works, the Westervelt equation is solved in Cartesian coordinates, and without a parabolic assumption. We overcame the numerical noise floor problem in conventional FDTD method by taking the difference between linear and nonlinear simulation results. The audible signal as well as higher harmonic signals are successfully extracted. The simulated acoustic signal gives correct predictions in both the spectrum and radiation pattern comparing with the measured signal. This new FDTD method can serve as a simulation tool for nonlinear acoustics. It also has potential to be a building block for a hybrid numerical simulation tool that use both beam-forming and FDTD scheme to simulate advanced parametric array form factors in real world applications.